IOPscience iopscience.iop.org

Home Search Collections Journals About Contact us My IOPscience

The crystal-field potential of solid C_{60} at room temperature

This article has been downloaded from IOPscience. Please scroll down to see the full text article.

1999 J. Phys.: Condens. Matter 11 2493

(http://iopscience.iop.org/0953-8984/11/12/004)

View the table of contents for this issue, or go to the journal homepage for more

Download details:
IP Address: 171.66.16.214
The article was downloaded on 15/05/2010 at 07:15

Please note that terms and conditions apply.

J. Phys.: Condens. Matter **11** (1999) 2493–2501. Printed in the UK PII: S0953-8984(99)94661-1

The crystal-field potential of solid C_{60} at room temperature

K Wulf†, P Schiebel†, W Prandl†, W Paulus‡ and G Heger§

† Institut für Kristallographie, Universität Tübingen, Charlottenstraße 33, D-72070 Tübingen, Germany

‡ Laboratoire Léon Brillouin, CE de Saclay, F-91191 Gif-sur-Yvette, France

§ Institut für Kristallographie, RWTH Aachen, Templergraben 55, D-52062 Aachen, Germany

Received 29 May 1998, in final form 28 December 1998

Abstract. Bragg intensities from neutron diffraction data for C_{60} single crystals were used to determine the rotational potential $V(\omega)$ at room temperature. The rotational potential is evaluated in terms of mixed rotator functions $\mathcal{M}$. The expansion coefficients v_l^ϵ, i.e. potential parameters, are obtained directly from experiment. The potential exhibits well developed minima, absolute ones at the Euler angle set ω_1 and relative ones at ω_2. They correspond to the two orientations, i.e. pentagonal and hexagonal facing, of the molecules in their low-temperature arrangement. The overall potential barrier height of the absolute minimum is 400 K and the difference between the two types of minima is 270 K.

1. Introduction

The carbon atoms of the C_{60} molecule form a regular truncated icosahedron [1] (figure 1). The C_{60} molecule exhibits full icosahedral symmetry as has been shown by NMR experiments [2]. In the solid state, C_{60} is a molecular crystal [3] and forms a face-centred-cubic (fcc) lattice with space group $Fm\bar{3}m$ [4], in which the C_{60} molecules are orientationally disordered at room temperature. C_{60} undergoes a phase transition at 250 K, in which the four molecules of the unit

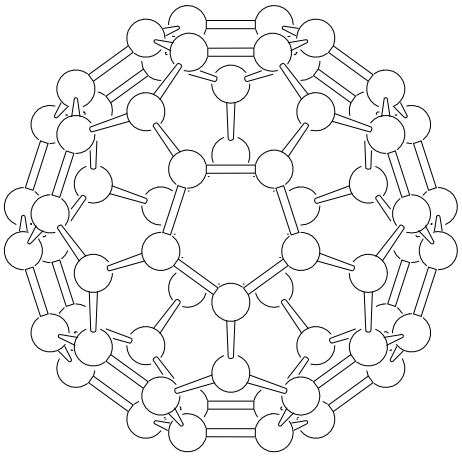

Figure 1. The C_{60} molecule.

 © 1999 IOP Publishing Ltd

cell of the fcc lattice become inequivalent. They align one of their threefold axes with one of the four crystal threefold axes and thus form a $Pa\bar{3}$ structure [5–7]. For the molecules there are two nearly degenerate equilibrium orientations, i.e. the pentagonal facing and hexagonal facing configurations. The former one is characterized by six pentagons facing the double bonds of neighbouring molecules, whereas in the latter one, which is energetically less favoured, six hexagons face the double bonds [7].

At room temperature the C_{60} molecules perform a three-dimensional rotational motion, which shows deviations from a free rotation [8, 9]. The orientational probability density function reveals two favoured orientations, which align a threefold molecular axis parallel to a threefold crystal axis [10]. Thus the low-temperature minimum-energy configurations are already present in the high-temperature phase.

For the understanding of the various properties of C_{60} it is essential to know the crystal-field potential of the C_{60} molecule in the solid state [11–14]. Therefore the construction of a reliable potential for the interaction of C_{60} molecules is an important problem and an increasing number of improved models of intermolecular interactions have been proposed, mainly based on the van der Waals type of interactions and electrostatic interactions [15–26].

Since the crystal field depends on the molecular structure, diffraction experiments allow one to obtain the effective crystal-field potential. In an earlier paper [10] we derived the total rotational potential $V(\omega)$ as calculated from the experimentally observed orientation distribution function $f(\omega)$. In the present paper we use new neutron data obtained for an untwinned crystal and determine $V(\omega)$ as a series expansion of rotator functions $\mathcal{M}$: these new results can be directly compared with data from interaction models [21–26].

2. Experimental procedure

The crystals used for our x-ray and neutron diffraction experiments were grown by sublimation [27]. The crystal for the x-ray experiment was almost spherical ($d = 0.2$ mm) and showed no detectable twins. The cubic lattice parameter was refined to 14.152(2) Å. A conventional four-circle Stoe diffractometer, equipped with a graphite (002) monochromator, was operated at a wavelength $\lambda_{\text{Mo K}\alpha} = 0.710\,73$ Å. Using ω–2θ scans, 1894 Bragg intensities were collected up to $(\sin\theta)/\lambda = 0.65$ Å^{-1}. This resulted in 205 unique reflections with an internal agreement factor $R_{\text{int}} = 0.039$.

In our neutron diffraction experiment we used a crystal with diameter 5 mm. In contrast to the samples in our previous study [10] this crystal showed no twins. The experiment was performed at the four-circle diffractometer 5C2 at the hot source of the Orphée reactor with a neutron wavelength of $\lambda = 0.8308(2)$ Å selected by a Cu(220) vertically focusing monochromator and a 0.25 mm thick erbium filter to reduce $\lambda/2$ contamination to less than 0.1%. The cubic lattice parameter was refined to 14.155(2) Å. Measurements were made up to $(\sin\theta/\lambda)_{\text{max}} = 0.81$ Å^{-1}; there were 300 unique reflections with an internal agreement factor of $R_{\text{int}} = 0.019$.

3. Theory

The structure factor of orientationally disordered molecular crystals is best formulated in terms of symmetry-adapted multipolar rotator functions [28,29]. In the literature, symmetry-adapted functions for the cubic and icosahedral point group [30–33] are available. This formalism was applied to C_{60} first by Michel and co-workers [11, 21–23, 25]. They use a coordinate system that differs from that selected by other authors and our choice.

The rotational part of the structure factor for a C_{60} crystal at room temperature is given by [10]

$$F_{\mathrm{rot}}(\boldsymbol{Q}) = 4\pi f_{\mathrm{X,N}}(\boldsymbol{Q}) \sum_{l\epsilon} \mathrm{i}^l j_l(Qr_{\mathrm{m}}) c_{l\epsilon} P_{l\epsilon}(\hat{\boldsymbol{Q}}) \tag{1}$$

where $f_{\mathrm{X,N}}$ is the x-ray structure factor or the neutron scattering length of the C atom, the j_l are spherical Bessel functions of order l and the $P_{l\epsilon}$ are symmetry-adapted spherical harmonics of the cubic point group $m\bar{3}m$ of the lattice site of the C_{60} molecule. Through the coefficients $c_{l\epsilon}$, the scattering density $W(\boldsymbol{r})$ on the sphere of the rotating C_{60} molecule with the radius r_{m} is given by

$$W(\boldsymbol{r}) = \frac{\delta(r - r_{\mathrm{m}})}{r^2} \sum_{l\epsilon} c_{l\epsilon} P_{l\epsilon}(\hat{\boldsymbol{r}}). \tag{2}$$

On the other hand, these coefficients are related to the orientational distribution function $f(\boldsymbol{\omega})$ [10]:

$$f(\boldsymbol{\omega}) = \sum_{l\epsilon\epsilon'} \frac{2l+1}{8\pi^2} \frac{c_{l\epsilon}}{\overline{\Pi}_{l\epsilon'}} \mathcal{M}^l_{\epsilon\epsilon'}(\boldsymbol{\omega}) \tag{3}$$

where the $\overline{\Pi}_{l\epsilon'}$ are the structural constants given in table 1 and the $\mathcal{M}^l_{\epsilon\epsilon'}$ are the symmetry-adapted rotator functions. We express the orientational distribution function $f(\boldsymbol{\omega})$ in terms of the rotational potential $V(\boldsymbol{\omega})$ using a Boltzmann factor:

$$f(\boldsymbol{\omega}) = \frac{\exp(-\beta V(\boldsymbol{\omega}))}{Z} \tag{4}$$

with the partition function:

$$Z = \int \exp(-\beta V(\boldsymbol{\omega}))\, \mathrm{d}\boldsymbol{\omega}. \tag{5}$$

The coefficients $c_{l\epsilon}$ can thus be expressed in terms of the rotational potential:

$$c_{l\epsilon} = \overline{\Pi}_{l\epsilon'} \int \mathcal{M}^l_{\epsilon\epsilon'}(\boldsymbol{\omega}) \exp(-\beta V(\boldsymbol{\omega}))\, \mathrm{d}\boldsymbol{\omega}. \tag{6}$$

On expanding the rotational potential in a series of symmetry-adapted rotator functions $\mathcal{M}$:

$$V(\boldsymbol{\omega}) = \sum_{l\epsilon\epsilon} V^l_{\epsilon\epsilon'} \mathcal{M}^l_{\epsilon\epsilon'}(\boldsymbol{\omega}) \tag{7}$$

the rotational part of the structure factor finally reads

$$F_{\mathrm{rot}}(\boldsymbol{Q}) = 4\pi f_{\mathrm{X,N}}(\boldsymbol{Q}) \times \sum_{l\epsilon} \mathrm{i}^l j_l(Qr_{\mathrm{m}}) P_{l\epsilon}(\hat{\boldsymbol{Q}}) \overline{\Pi}_{l\epsilon'} \int \mathcal{M}^l_{\epsilon\epsilon'}(\boldsymbol{\omega}) \exp\left(-\beta \sum_{l'\epsilon\epsilon} V^{l'}_{\epsilon\epsilon'} \mathcal{M}^{l'}_{\epsilon\epsilon'}(\boldsymbol{\omega})\right) \mathrm{d}\boldsymbol{\omega}. \tag{8}$$

Thus the potential parameters can be directly extracted from the single-crystal data and we avoid the difficulties with the high-temperature expansion of Boltzmann factors encountered as soon as the condition $|V(\boldsymbol{\omega})|/kT \ll 1$ is not obeyed. The integrals in (8) are evaluated numerically.

Table 1. The structural constants $\overline{\Pi}_{l\epsilon'}$ up to order $l = 22$. ϵ' is 1 for all of the l used.

l	0	6	10	12	16	18	20	22
$\overline{\Pi}_{l\epsilon'}$	16.93	2.56	−19.35	−7.88	−17.94	38.21	−17.10	−2.96

4. Results and discussion

The coefficients of the rotational potential in solid C_{60} are fitted to the experimental neutron scattering data using (8). The fitting procedure used potential parameters $V^{l'}_{\epsilon\epsilon'}$ up to order $l' = 18$, whereas the number density in the first sum of equation (8) was evaluated up to order $l_c = 22$. Neither increasing l_c nor using more potential parameters resulted in better R-values. The results of the refinements are shown in table 2.

Table 2. Results of the refinement of the potential parameters $V^{l}_{\epsilon\epsilon'}$ at room temperature. Potential parameters are given in K.

	Neutron	X-ray
c_{ext}	0.0117(7)	0.010(1)
u (Å^2)	0.0150(3)	0.0187(4)
r (Å)	3.5470(5)	3.5388(4)
$V^{6}_{1,1}$	224(39)	413(35)
$V^{10}_{1,1}$	69(8)	52(9)
$V^{12}_{1,1}$	42(35)	57(36)
$V^{12}_{2,1}$	328(27)	305(36)
$V^{16}_{1,1}$	30(24)	−22(38)
$V^{16}_{2,1}$	51(22)	33(33)
$V^{18}_{1,1}$	−1(17)	6(23)
$V^{18}_{2,1}$	−72(12)	−19(15)
R	0.069	0.054
R_w	0.028	0.018
N_{hkl}	300	205

$$R = \left(\sum_{hkl} ||F_o^{hkl}| - |F_c^{hkl}||\right) \Big/ \left(\sum_{hkl} |F_o^{hkl}|\right)$$

$$R_w = \left[\left(\sum_{hkl} w(|F_o^{hkl}| - |F_c^{hkl}|)^2\right) \Big/ \left(\sum_{hkl} w(F_o^{hkl})^2\right)\right]^{1/2}$$

The crystal-field coefficient $V^{12}_{2,1}$ is the most prominent. The main features of the potential are determined by the functions of order $l = 6$, and $l = 12$ with $\epsilon = 2$. This latter index refers to the second allowed symmetry-adapted spherical harmonic $P_{l\epsilon}$ of the cubic point group $m\bar{3}m$ [32].

Figure 2(a) shows a one-dimensional cut through the Euler space along $\omega_1 = (45^\circ, \beta, 0^\circ)$ through the potential $V(\omega)$ derived from the x-ray and neutron data. Along this path the potential shows two minima (out of 240 symmetry-equivalent ones in the whole Euler space) with a potential difference of ≈300 K, while the overall potential height amounts to ≈450 K (figure 2), corresponding to the values found in [10]. Again the potential minima appear at the Euler angles $\omega_1 = (45^\circ, 87.89^\circ, 0^\circ)$ and $\omega_2 = (45^\circ, 17.36^\circ, 0^\circ)$. Both orientations align a threefold axis, a twofold axis and a mirror plane of the molecule with corresponding symmetry elements of the cubic crystal surrounding. Figures 2(b), 2(c) show $V(\omega)$ together with the most important contributions $V^{6}_{1,1}$ and $V^{12}_{2,1}$. These figures demonstrate that ω_1 and ω_2 are determined by the symmetry properties of $V^{12}_{2,1}$. In addition, the shape of the absolute potential

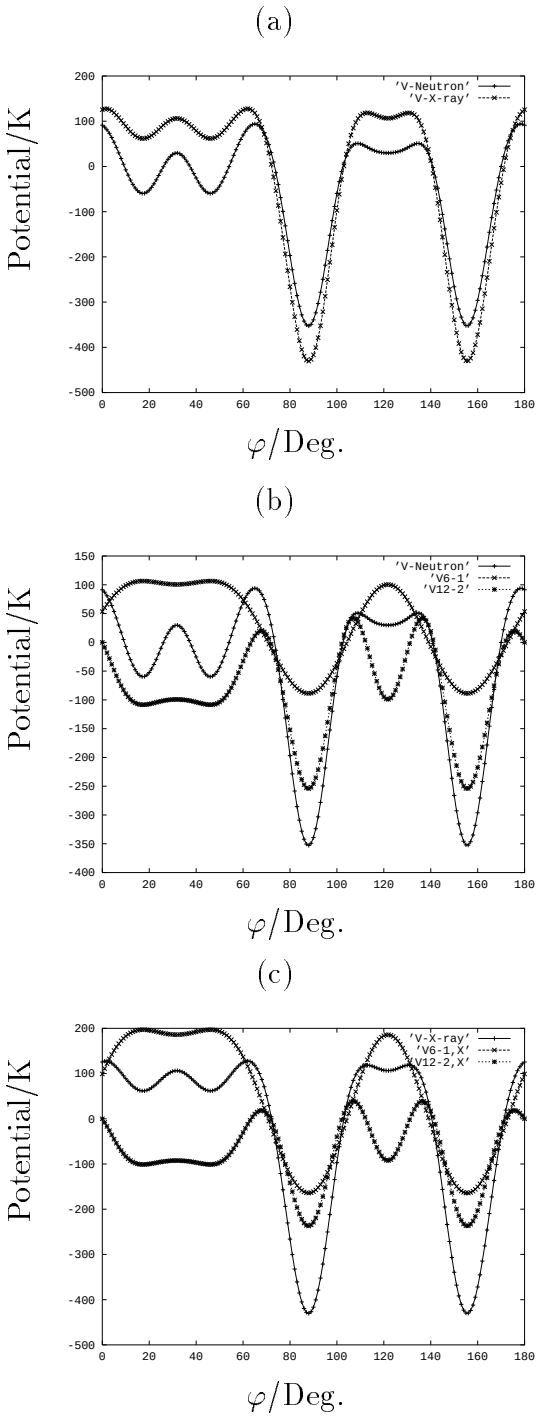

Figure 2. A one-dimensional cut through the Euler space: the rotational potential with $\alpha = 45^\circ$ and $\gamma = 0^\circ$. The potential minima are clearly visible at $\beta_1 = 87.89^\circ$ and $\beta_2 = 17.36^\circ$. (a) The potential derived from the x-ray and neutron data. (b) The main contributions to the potential from neutron data. (c) The main contributions to the potential from x-ray data.

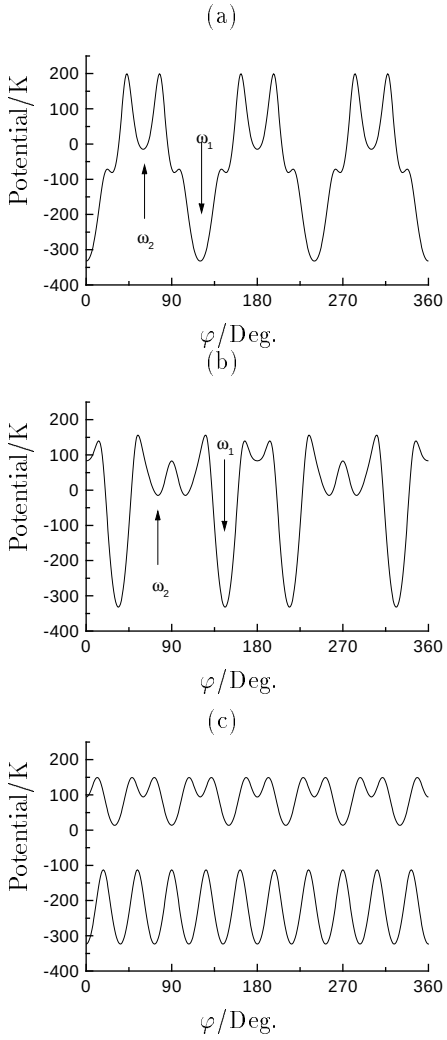

Figure 3. The rotational potential at room temperature for uniaxial rotations with $0^\circ \leqslant \varphi < 360^\circ$ with (a) the threefold molecular axis parallel to a threefold crystal axis, (b) a twofold molecular axis parallel to a twofold crystal axis and (c) a threefold (top) and a fivefold (bottom) molecular axis parallel to a twofold crystal axis.

minimum $V(\omega_1)$ is dominated by $V^{12}_{2,1}$, whereas $V^{6}_{1,1}$ and $V^{12}_{2,1}$ add to the potential difference between $V(\omega_1)$ and $V(\omega_2)$.

Figure 3 shows the potential derived from the neutron data for some uniaxial rotations: rotations around a threefold molecular axis parallel to a threefold crystal axis or a twofold molecular axis parallel to a twofold crystal axis reach both potential minima, but only by surmounting nearly the full potential barrier. A rotation around a fivefold axis parallel to a twofold crystal axis has minima slightly above the overall potential minima, but the barrier between those minima amounts to only 200 K.

Figures 2 and 3(a)–3(c) are nearly identical to the corresponding figures in our previous paper [10] in which $V(\omega)$ was determined as $V(\omega) = -kT \ln f(\omega)$. They demonstrate clearly

that the potential is independent of the description and allow for a comparison with results published previously. With the analytical method that we used earlier [10], only the total $V(\omega)$ was calculated. Here, however, we break down $V(\omega)$ into the basic orthogonal components $V^l_{\epsilon,\epsilon'}\mathcal{M}^l_{\epsilon,\epsilon'}$. This allows a direct comparison of theoretical model potentials with observed ones.

Table 3. c-coefficients calculated from the potential parameters given in table 2 according to (6).

	Neutron	X-ray
$c_{0,1}$	1.0000	1.0000
$c_{6,1}$	−0.0106	−0.0183
$c_{10,1}$	0.0111	0.0132
$c_{12,1}$	0.0048	0.0046
$c_{12,2}$	0.0266	0.0274
$c_{16,1}$	−0.0091	−0.0138
$c_{16,2}$	0.0078	0.0066
$c_{18,1}$	−0.0010	−0.0027
$c_{18,2}$	0.0257	0.0218
$c_{20,1}$	0.0016	0.0014
$c_{20,2}$	0.0079	−0.0051
$c_{22,1}$	0.0006	0.0001
$c_{22,2}$	0.0000	0.0000

In addition, we calculated the c-coefficients corresponding to the refined potential parameters using equation (6) (table 3). The values obtained from our new neutron data set, which is based on a better crystal, fit very well to those obtained from the data sets for the two other crystals. The values for the x-ray data are identical, within error bars, to the ones obtained previously, demonstrating the equivalence of the analysis (table 3). They agree with the experimentally obtained c-coefficients available in the literature, as summarized in table 4.

Table 4. Comparison of c-coefficients obtained from experimental data; $c_{0,1} = 1$

	N3, present data	N2, Schiebel *et al* [10]	N1, Chow *et al* [8]	X, David *et al* [9]	X	N powder
$c_{6,1}$	−0.011(1)	−0.014(1)	−0.008(2)	−0.018(1)	−0.023(2)	−0.023(7)
$c_{10,1}$	0.011(2)	0.014(2)	0.010(2)	0.013(1)	0.013(1)	0.021(3)
$c_{12,1}$	0.005(2)	0.006(3)	0.003(2)	0.005(2)	0.009(2)	0.013(4)
$c_{12,2}$	0.027(2)	0.031(3)	0.029(3)	0.027(2)	0.026(1)	0.042(4)
$c_{16,1}$	−0.009(3)	−0.009(6)	−0.024(5)	−0.013(3)	−0.008(2)	−0.014(8)
$c_{16,2}$	0.008(2)	0.002(5)	0.010(4)	0.007(3)	−0.000(2)	−0.020(14)
$c_{18,1}$	−0.001(3)	−0.006(7)	0.001(2)	−0.003(3)	−0.003(2)	−0.014(28)
$c_{18,2}$	0.026(3)	0.026(6)	0.010(5)	0.020(3)	0.024(2)	0.054(13)

Table 5. Calculated values for the c-coefficients; $c_{0,1} = 1$.

	Lamoen and Michel [21]	Lamoen and Michel [23]	Savin *et al* [26]
$c_{6,1}$	−0.008	−0.025	−0.004
$c_{10,1}$	0.038	0.050	0.013
$c_{12,1}$	0.003	0.002	0.003
$c_{12,2}$	0.014	0.035	0.011

Table 6. Calculated V-coefficients. Column 1: V-coefficients calculated from the c-coefficients published by Savin *et al* [26]. Columns 2 to 4: V-coefficients calculated by Lamoen and Michel. Due to the difference in the choice of the coordinate system, their values for $V^{10}_{1,1}$, $V^{12}_{1,1}$, $V^{12}_{2,1}$ have been multiplied by -1 to make them fit to the conventions used in the present paper.

	[26]	[21], disordered	[23], disordered	[25], ordered
$V^{6}_{1,1}$	109	198.42	470.34	383.94
$V^{10}_{1,1}$	71	206.91	172.18	194.48
$V^{12}_{1,1}$	42	46.94	77.31	90.51
$V^{12}_{2,1}$	181	230.40	347.89	412.46

Tables 5 and 6 give c-coefficients and crystal-field coefficients calculated on the basis of microscopic models. Michel and co-workers used a high-temperature expansion to derive c-coefficients from calculated V-coefficients [21–23, 25]:

$$c_{l\epsilon} = \frac{\bar{\Pi}_{l,\epsilon'} V^{l}_{\epsilon\epsilon'}}{T(2l+1)}. \tag{9}$$

This high-temperature expansion was also applied by other authors to compare their calculated V-coefficients to experimental data [26].

However, applying the high-temperature expansion to our V-coefficients does not result in the c-coefficients of table 3. This may be understood from figure 2, where it is obvious that the potential barriers amount to roughly 300 K. Therefore the condition for the application of the high-temperature expansion, i.e. $\Delta V/kT \ll 1$, is not rigorously fulfilled, and so the integrals in (8) cannot be solved correctly by expanding the Boltzmann factor and then using the orthogonality of the $\mathcal{M}$-functions.

The progress in our present work is that now a parametrization of the rotational potential in terms of symmetry-adapted functions is available. These coefficients may also be derived from theoretical calculations based on intermolecular potentials. Thus our work may serve as a reference for the choice of the most appropriate potential description. A detailed comparison of six model potentials with the experimentally determined potentials [8–10] published up to 1997 has been given by Launois *et al* [13]. Their analysis demonstrates that the model (LM) due to Lamoen and Michel [21] describes the experimental data reasonably well with two limitations: the barrier height of the LM potential for a rotation of the molecular 6-axis about a crystal 3-axis amounts to only 50% of the observed potential [10] and, second, the data evaluation requires uniquely the inclusion of a term with $l = 18$ in the calculation of $f(\omega)$, and also the corresponding contributions which enter into $V(\omega)$. This is proved uniquely by our present analysis. The absolute value of $V^{18}_{2,1} = 72$ K is well beyond the computed error 12 K.

Acknowledgments

We acknowledge financial support of this investigation by the BMBF and the DFG.

References

[1] Kroto H W, Heath J R, O'Brien S C, Curl R F and Smalley R E 1985 *Nature* **318** 162
[2] Johnson R D, Yannoni C S, Dorn H C, Salem J R and Bethune D S 1992 *Science* **255** 1235
[3] Krätschmer W, Lamb L D, Fostiropoulus K and Huffman R 1990 *Nature* **347** 354

[4] Fleming R M, Siegrist T, Marsh P M, Hessen B, Kortan A R, Murphy P W, Haddon R C, Tycko R, Dabbagh G, Mujsce A M, Kaplan M L and Zahmak S M 1991 *Mater. Res. Soc. Symp. Proc.* **206** 691
[5] Heiney P A, Fischer J E, McGhie A R, Romanow W J, Denenstein A M, McCauley J P Jr, Smith A B and Cox D E 1991 *Phys. Rev. Lett.* **66** 2911
[6] Heiney P A 1991 *Phys. Rev. Lett.* **67** 1468
[7] David W I F, Ibberson R M, Dennis T J S, Hare J P and Prassides K 1992 *Europhys. Lett.* **18** 219
[8] Chow P C, Jiang X, Reiter G, Wochner P, Moss S C, Axe J D, Hanson J C, McMullan R K, Meng R L and Chu C W 1992 *Phys. Rev. Lett.* **69** 2943
[9] David W I F, Ibberson R M and Matsuo T 1993 *Proc. R. Soc.* A **442** 129
[10] Schiebel P, Wulf K, Prandl W, Heger G, Papoular R and Paulus W 1996 *Acta Crystallogr.* A **52** 176
[11] Copley J R D and Michel K H 1993 *J. Phys.: Condens. Matter* **5** 4353
[12] Axe J D, Moss S C and Neumann D A 1994 *Solid State Physics* vol 48, ed H E Ehrenreich and F Spaepen (New York: Academic) pp 149–224
[13] Launois P, Ravy S and Moret R 1997 *Phys. Rev.* B **55** 2651
[14] Launois P, Ravy S and Moret R 1995 *Phys. Rev.* B **52** 3414
[15] Guo Y, Karasawa N and Goddard W A III 1991 *Nature* **351** 464
[16] Cheng A and Klein M L 1992 *J. Phys. Chem.* **96** 2027
[17] Sprik M, Cheng A and Klein M L 1992 *J. Chem. Phys.* **96** 2027
[18] Lu J P, Li X P and Martin R M 1992 *Phys. Rev. Lett.* **68** 1551
[19] Burgos E, Halac E and Bonadeo H 1993 *Phys. Rev.* B **47** 13 903
[20] Heid R 1993 *Phys. Rev.* B **48** 807
[21] Lamoen D and Michel K H 1993 *Z. Phys.* B **47** 15 912
[22] Lamoen D and Michel K H 1993 *Phys. Rev.* B **48** 807
[23] Lamoen D and Michel K H 1994 *J. Chem. Phys.* **101** 1435
[24] Pintschovious L and Chaplot S L 1995 *Z. Phys.* B **98** 527
[25] Michel K H, Lamoen D and David W I F 1996 *Acta Crystallogr.* A **51** 365
[26] Savin S, Harris A B and Yıldırım T 1997 *Phys. Rev.* B **55** 14 182
[27] Haluška M, Kuzmany H, Vybornov M, Rogl P and Fejdi P 1993 *Appl. Phys.* A **56** 161
[28] Press W and Hüller A 1973 *Acta Crystallogr.* A **29** 252
[29] Prandl W 1981 *Acta Crystallogr.* A **37** 811
[30] Laporte O 1948 *Z. Naturf.* a 447
[31] Cohan N V 1958 *Proc. Cambridge Phil. Soc.* **54** 28
[32] Altmann S L and Cracknell A P 1965 *Rev. Mod. Phys.* **37** 19
[33] Prandl W, Schiebel P and Wulf K 1996 *Acta Crystallogr.* A **52** 171